Stem Cell Reports, Volume *7*

Supplemental Information

Identification and Characterization of the Dermal Panniculus Carnosus Muscle Stem Cells

Neia Naldaiz-Gastesi, María Goicoechea, Sonia Alonso-Martín, Ana Aiastui, Macarena López-Mayorga, Paula García-Belda, Jaione Lacalle, Carlos San José, Marcos J. Araúzo-Bravo, Lidwine Trouilh, Véronique Anton-Leberre, Diego Herrero, Ander Matheu, Antonio Bernad, José Manuel García-Verdugo, Jaime J. Carvajal, Frédéric Relaix, Adolfo Lopez de Munain, Patricia García-Parra, and Ander Izeta

SUPPLEMENTAL RESULTS

Transcriptomic analyses confirm the myogenic identity of *Myf5+* dermal precursor cells. To understand if myogenic precursors arise during dermal sphere culture or where otherwise present in the original dissociated tissue sample, transcriptomic analyses were performed in *Myf5*^{Sor} positive cell-derived sphere cultures and the appearance of myogenic genes at day 7 of proliferation culture as compared to day 0 was analyzed (Figure S6). A principal component analysis (PCA) of gene expression data of 78 arrays corresponding to 35 cell different populations (as detailed in Table S2) showed that all dermis-derived samples (myogenic and non-myogenic) clustered together with known myogenic samples but also with fibroblasts and adipocytes (Figure S6A). Pairwise comparisons showed that, of the 4,735 genes differentially expressed between these samples, 52 probes (15 genes) were associated with the GO category "Satellite Cell" and 154 probes (63 genes) classified under "Striated Muscle Cell Differentiation". Analyses of these myogenic probes/genes showed that activated satellite/immature myoblast markers such as *Musk* (DeChiara et al., 1996), *Myod1*, *Shh* (Voronova et al., 2013), *Igfbp5* (Sharples et al., 2011) and *Bmp4* (Dahlqvist et al., 2003; Ono et al., 2011) were preferentially expressed at day 0 sphere cultures. In contrast, committed/differentiated myoblast genes such as *Cdh2* (Lovett et al., 2006), *Rara/Rarb* (Halevy and Lerman, 1993), *Myh3*, *Kcnh1* (Rozwadowska et al., 2013; Stern-Straeter et al., 2009) and *Myf6* (Sambasivan et al., 2013) were upregulated at day 7 (Figure S6, B-C). These data suggested that activated PC satellite cells were expanding and differentiating in dermal sphere cultures.

Dermal myogenic fractions branched together and separate from non-myogenic (*Cspg4+*) fraction when hierarchical clustering of samples was performed using the correlation metric and the average linkage method (Figure S7A). To further discriminate, differentially expressed genes with a FC>2 in a log2 scale between myogenic and non-myogenic (*Cspg4+*) dermal samples were determined. As expected, key myogenic factors such as *Myod1, Myf6, Ttn* and *Myog* were downregulated in the dermal non-myogenic fraction (*Cspg4+*) when compared to the dermal myogenic fractions (Figure S7B). Furthermore, of the 1,476-3,397 genes upregulated when compared to *Cspg4+* dermal cells, the dermal myogenic and other myogenic samples obtained from public databases shared 1,000 genes (Figure S7C). Finally, gene set enrichment analysis (GSEA) of molecular signatures showed two muscle development categories among the significant GSEA-enriched terms (Figure S7D). In all, transcriptomic data are compatible with dermal myogenic precursor cells being of muscle origin.

SUPPLEMENTAL MATERIALS AND METHODS

Generation of the new *B195AP-Cre* line. The *B195APZ* BAC construct was modified by recombineering (Swaminathan et al., 2001) with modifications as described previously (Carvajal et al., 2008). BAC clones were transferred into DY380 cells (kindly provided by Neil Copeland, National Cancer Institute-Frederick, Frederick, Maryland), which carry the temperature-inducible lambda-recombinase system. Briefly, 250bp homology arms were generated by PCR and joined to *Cre*. The construct was electroporated into electrocompetent DY380 cells carrying the *B195APZ* construct and used to replace the *nlacZ* gene by the *Cre* gene. Pools of 20-30 clones were screened by PCR and positive pools further diluted to single cells in order to identify correctly targeted clones. Full details on the targeting constructs can be obtained on request. BAC DNA was prepared using the QIAgen Maxiprep kit (Qiagen) as described previously (Carvajal et al., 2001), dialyzed against BAC microinjection buffer (10 mM Tris-HCl pH 7.5, 0.1 mM EDTA pH 8.0, 100mM NaCl), diluted to 1.6 ng/ml in BAC microinjection buffer and used to inject day 0 fertilized mouse eggs from CBA/Ca × C57Bl/6 crosses. For the generation of this new line, experimentation was performed according to United Kingdom Home Office Regulations and current Spanish legislation (RD53/2013) on animal experimentation.

Skin histology for inmunofluorescence. Murine dorsal skin fragments of approximately 0.5 cm2 were excised, and were directly embedded in OCT (Sakura) and frozen in isopentane (Merck) cooled in liquid nitrogen or pre-fixed in fixative solution (Histofix; Histolab) at 4ºC overnight. Fixed samples were immersed in 5% sucrose at 4ºC for 5 hours and in 30% sucrose at 4ºC overnight. The next day, samples were embedded in OCT, and immediately frozen in isopentane cooled in liquid nitrogen. Seven µm cryostat transverse sections were fixed in cold methanol for 3 min or in 4% paraformaldehyde 10 min, incubated in 0,1% Triton in PBS for 20 minutes, and followed by 10% goat serum for 30 min or with 10% BSA solution 1 hour. Primary antibodies were incubated for 1h at RT or O/N at 4ºC, and then incubated with secondary antibodies (see supplementary data) for 1h at RT. The samples were stained with Hoechst, washed 3 times with phosphate buffered saline (PBS) and once with distilled water and with milliQ water, and then mounted with Fluoro-Gel (Electron Microscopy Sciences). The samples were examined under epifluorescence microscope (Eclipse TS100) or Zeiss LSM 510 Meta confocal microscope.

Immunofluorescence and microscopy. Cells were fixed in 4% paraformaldehyde (PFA; Electron Microscopy Sciences) for 10 min at room temperature (RT) and then they were permeabilized/blocked by using 0.3% Triton X-100 in PBS (PBST) plus 5% normal donkey serum (Sigma-Aldrich) for 1h at RT. Cells were incubated with the appropriate primary antibody diluted in PBST for 2h at RT (as detailed below). After that, cells were incubated for 1h at RT with the appropriate secondary antibody diluted in PBST (detailed in Supplementary data). Prior to mounting in Vectashield (Vector Laboratories), cells were counterstained with 10 µg/ml Hoechst 33258 (Sigma-Aldrich) for 2 min at RT. Fluorescence images were obtained by using a Nikon Eclipse 80i microscope coupled to Nikon Digital Sight and analyzed with Nikon NIS-Elements Advance Research software. Primary antibodies used were anti-myogenin (Myog) (F5D; 1:50; Developmental Studies Hybridoma Bank, DSHB), anti-myosin heavy chain (MyHC) (A4.1025, all fibers; 1:50; DSHB), goat anti-GFP (GFP) (ab6673; 1:500; Abcam), chicken anti-GFP (GFP) (ab13970; 1:500; Abcam), anti-DsRed (DsRed) (632496; 1:100; Clontech) and anti-Laminin (L9393, Sigma-Aldrich). Secondary antibodies used were donkey anti-goat Alexa Fluor 488 (A11055; 1:500; Invitrogen), donkey anti-mouse Alexa Fluor 555 (A31570; 1:500; Invitrogen), donkey anti-rabbit Alexa Fluor 555 (A31572; 1:500; Invitrogen), Alexa fluor 594-conjugated goat anti-rabbit (A11012) and goat anti-chicken DyLight® 488 (ab96947; 1:500; Abcam).

Transmission electron microscopy (TEM). After fixation in 3.5% glutaraldehyde (Electron Microscopy Sciences), cell cultures were washed in 0.1 M PBS (pH 7.4) and treated with 2% osmium tetraoxide (Electron Microscopy Sciences) in 0.1 M PBS (pH 7,4) for 2h at RT. Samples were rinsed, dehydrated through increasing ethanol solutions and stained in 2% uranyl acetate (Electron Microscopy Sciences) at 70% ethanol. Dehydrated cell cultures were embedded in araldite (Fluka). Semithin sections (1.5µm-thick) were cut with a diamond knife and stained with 1% toluidine blue solution (Sigma-Aldrich), re-embedded for ultrathin (70 nm-thick) sectioning, and examined under a Tecnai-Spirit Electron Transmission Microscope (TEM) coupled to a Morada TEM CCD camera (Soft Imaging System).

β-Galactosidase reporter gene staining and Alkaline Phosphatase reporter gene staining. LacZ staining was performed using the β-Galactosidase Reporter Gene Staining Kit (GALS; Sigma-Aldrich). Skin fragments were fixed in 4% paraformaldehide (PFA) for 40 min at 4°C. After

incubation in X-gal solution for 3h at 37°C, samples were washed, dehydrated with increasing sucrose concentration (10-20%) for 3 hours, embedded in OCT and frozen in liquid nitrogen-cooled isopentane (Merck). Sixty cryostat sections were cut, mounted in glycerol and examined under the microscope. Alkaline Phosphatase (AP) reporter gene staining was performed using the Alkaline Phosphatase Blue Membrane Substrate Solution (AB0300-1KT; Sigma-Aldrich). Skin fragments were fixed in 4% paraformaldehyde in PBS O/N at 4°C, rinsed twice in PBS supplemented with 2 mM MgCl2 (PBSMg), and washed in PBSMg for 10 minutes. Endogenous phosphatases were inactivated by incubation for 1 hour in PBSMg at 65°C. Samples were washed in ice-cold AP-buffer (100 mM Tris-HCl pH 9.5, 100 mM NaCl, 50 mM MgCl2, 0.1% Tween 20) and AP-buffer, transferred to AP-staining buffer and stained for 40 min in the dark at 4°C. The reaction was stopped by washing the tissue samples in ice-cold PBS in the dark at 4°C for 16 hours, dehydrated with increasing sucrose concentration (10-20%) for 3 hours, embedded in OCT and frozen as above. Sixty cryostat sections were cut, mounted in glycerol and examined under the microscope. For β-Galactosidase staining on whole-mount mouse embryos, these were fixed overnight in Mirsky's fixative (National Diagnostics) at 4°C, washed three times in PBSA (Ca++, Mg++-free phosphate-buffered saline)/0.02% Nonidet P-40 for 20 min at room temperature, placed in 7-10 ml of X-gal solution [5 mM K3Fe(CN)6, 5 mM K4Fe(CN)6 • 3H2O, 2 mM MgCl2, 0.02% Nonidet P-40, 0.4 mg/ml X-Gal in PBSA] for 2–6 h (depending on stage) at 37°C, and post-fixed in Mirsky's fixative.

Flow cytometry and cell sorting. Cultured spheres were dissociated with 0.25% Trypsin-EDTA (Sigma) for 5 min at 37ºC, PBS-washed, filtered through a 70 µm cell strainer, counted, and resuspended in PBS without Ca^{++} and Mg^{++}, with BSA 0.5%, 25mM HEPES and 5mM EDTA (sorting buffer; pH=7.2). For flow cytometry assays of YFP, data were acquired on a BD FACSCantoA flow cytometer using blue excitation and collecting fluorescent signals on the 530/30 (YFP) band pass filter. Tomato and GFP expression data were acquired on BD FACSAria III cell sorter using blue and yellow-green excitation and collecting fluorescent signals on the 530/30 (GFP) and 610/20 (TdTomato) band pass filters. Data acquisition was done for both assays with FACSDiva Software using control littermate mice to adjust setting parameters. Sample data were analyzed excluding doublets and non-viable cells (To-Pro-3 positive cells), with BD FACS diva software and FlowJo. Data are represented as dot plots showing green fluorescence (EYFP or EGFP) vs. orange fluorescence (autofluorescence).

Syndecan-4-based cell sorting. Cultured dermospheres were pelleted and dissociated with 0.25% Trypsin-EDTA (Sigma) for 5 min at 37°C, PBS-washed, filtered through a 70 µm cell strainer, and counted. Cells were blocked with PBS with BSA 1% and FBS 10% for 10 min at room temperature. The primary antibody, Biotin Rat Anti-Mouse Syndecan-4 (IgG2a) (550351; 1µg/test; BD Biosciences), and isotype, Biotin Rat IgG2a,κ Isotype Control (553928; 1µg/test; BD Biosciences) were added and incubated for 30 min at 4ºC. The cells were washed with PBS with BSA 1%, incubated with APC Streptavidin (554067; 0.2mg/ml; BD Biosciences) for 30 min at 4ºC, washed again, and re-suspended in PBS without Ca^{++} and Mg^{++}, with BSA 0.5%, 25mM HEPES and 5mM EDTA (sorting buffer; pH=7.2) onto 5 ml polypropylene tubes. Auto-fluorescence was adjusted with the *wt* mice. PMT settings were established on live singlets by using unstained cells. Non-specific bindings were evaluated with the corresponding isotypic controls used at the same concentration, same isotype and same fluorophore that the antibody of interest. Sorting experiments were done on a FACSAria III cell sorter (BD Biosciences), at low sheath pressure (20 psi) using 100 µm nozzle. Sorting procedures were done excluding dead cells (with either 7AAD or Sytox Green) and doublets; sorted cells were collected on proliferation medium without serum.

Gene expression. Total RNA was extracted from cells by miRNeasy Mini kit (Qiagen) and converted into complementary DNA with the High-Capacity cDNA Reverse Transcription Kit (Applied Biosystems). Real-time quantitative PCR (qRT-PCR) analysis was carried out using Taqman gene expression assays in the 7900 HT Fast Real-Time PCR System (Applied Biosystems). Each cDNA sample was amplified in triplicates. The cycling conditions were 95ºC/10 min followed by 40 cycles at 95ºC/15 s, 60ºC/1 min in a reaction mixture that contained 1x Taqman Universal PCR Master Mix and 1x Assay Mix in a final volume of 20µl. The relative quantity of the gene targets was determined by the 2ΔΔCt method (Livak and Schmittgen, 2001) using Tbp as a housekeeping control.

Transcriptomic analysis. Total RNA was extracted (DNA-free) from FACS-sorted cells pooled from 8-10 animals per strain, by using miRNeasy Micro Kit (217084, Qiagen). RNAs were controlled using Nanodrop ND-1000 and Bioanalyzer 2100 Expert from Agilent, then 25 ng of RNA was used as input for labeled cRNA synthesis with the Low Input Quick Amp Labeling Kit (5190-2305, Agilent

Technologies) and the One-color microarray-based gene expression protocol, according to manufacturer´s instructions. Labeled cRNAs were hybridized to Agilent SurePrint G3 Mouse GE 8x60K Microarray Kit (G4852A, Agilent Technologies). The slides were scanned on a Tecan scanner MS200 and analyzed by Feature Extraction V.11.5.1.1.

Molecular signature enrichment analysis. The molecular signatures were taken from the gene set collection C5 of the version 3.0 of the Molecular Signatures Database (MSigDB) (Subramanian et al., 2005). The significance of the gene set of the different expressed genes was analyzed using an enrichment approach based on the hypergeometric distribution. The significance (p-value) of the gene set enrichment was calculated using the hypergeometric distribution. The multitest effect influence was corrected trough controlling the false discovery rate using the Benjamini-Hochberg correction at a significance level $\alpha=0.05$.

SUPPLEMENTAL FIGURES AND LEGENDS

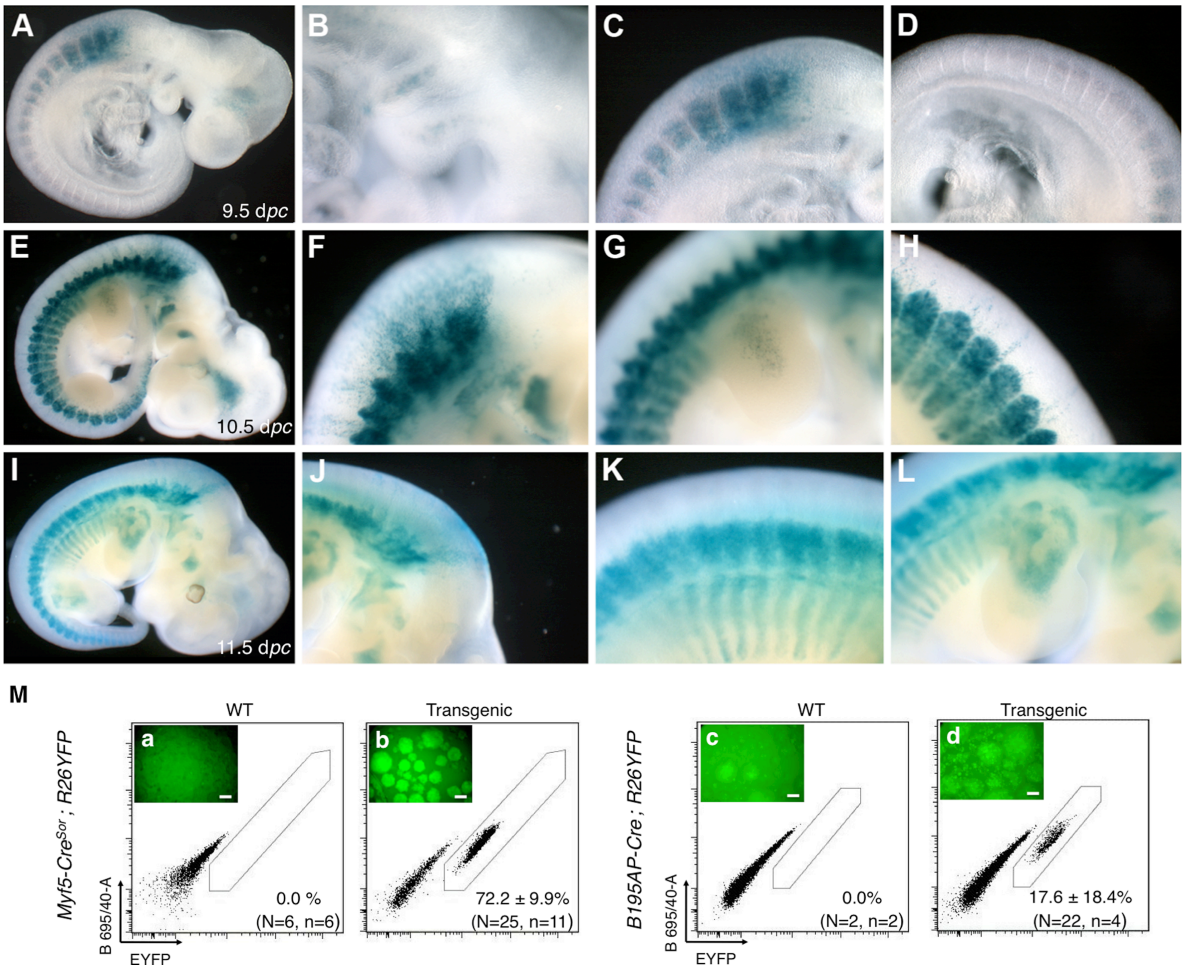

Figure S1. Time course of embryos carrying the *Myf5* reporter construct *B195AP-Cre* crossed with the *R26LACZ* strain, related to Figure 1. Representative mouse embryos (A, E, I) and close-ups from the same embryos (B-D, F-H, J-L) at 9.5d*pc* (A-D), 10.5d*pc* (E-H) and 11.5d*pc* (I-L). (A) β-Galactosidase staining can be detected at the known sites of *Myf5* expression at 9.5d*pc*, including the (B) mandibular and hyoid arches, (C) cervical somites and (D) the remaining somites with the exception of the 3 or 4 most recently formed; this apparent delay is likely caused by the time required to generate high levels of CRE protein in order to recombine the *R26LACZ* locus. (E) At 10.5d*pc* *Myf5+* cells can be detected in all muscle progenitor cells known to express *Myf5* at this stage, including all somites, branchial arches, hypoglossal chord and brain. (F) Interestingly, large numbers of *Myf5+* cells appear to migrate dorsally, into non-typical skeletal muscle locations. (G) *Myf5+* cells are also clearly visible in the forelimbs. (H) Migrating cells are not restricted to cervical positions but appear throughout the embryo but at positions always dorsal to the somites; note

that while migration in cervical positions does not follow any apparent pattern, migration at more caudal positions follows straight lines. (I) By 11.5dpc, most *Myf5+* cells are restricted to defined skeletal muscle locations such as the thoracic muscles, fore and hindlimb muscles, mandibular and hyoid arch derivatives. (J, K) Cells continue to migrate dorsal to the somites. (L) Detail of *Myf5+* cells in the forelimb. (M) Comparative analysis of EYFP+ cells by fluorescence and quantification by flow cytometry in dermal spheres isolated from *Myf5*^{SOR} and *B195AP* lineage tracing models. Left panels (a, c) show WT animal controls and right panels (b, d) transgenic animals. Insets, fluorescence images of dermal sphere cultures showing EYFP expression restricted to the transgenic animals. (Scale bars, 100 µm). Numbers represent mean±SD. The experiments were independently replicated as specified (N=mice; n=experiments).

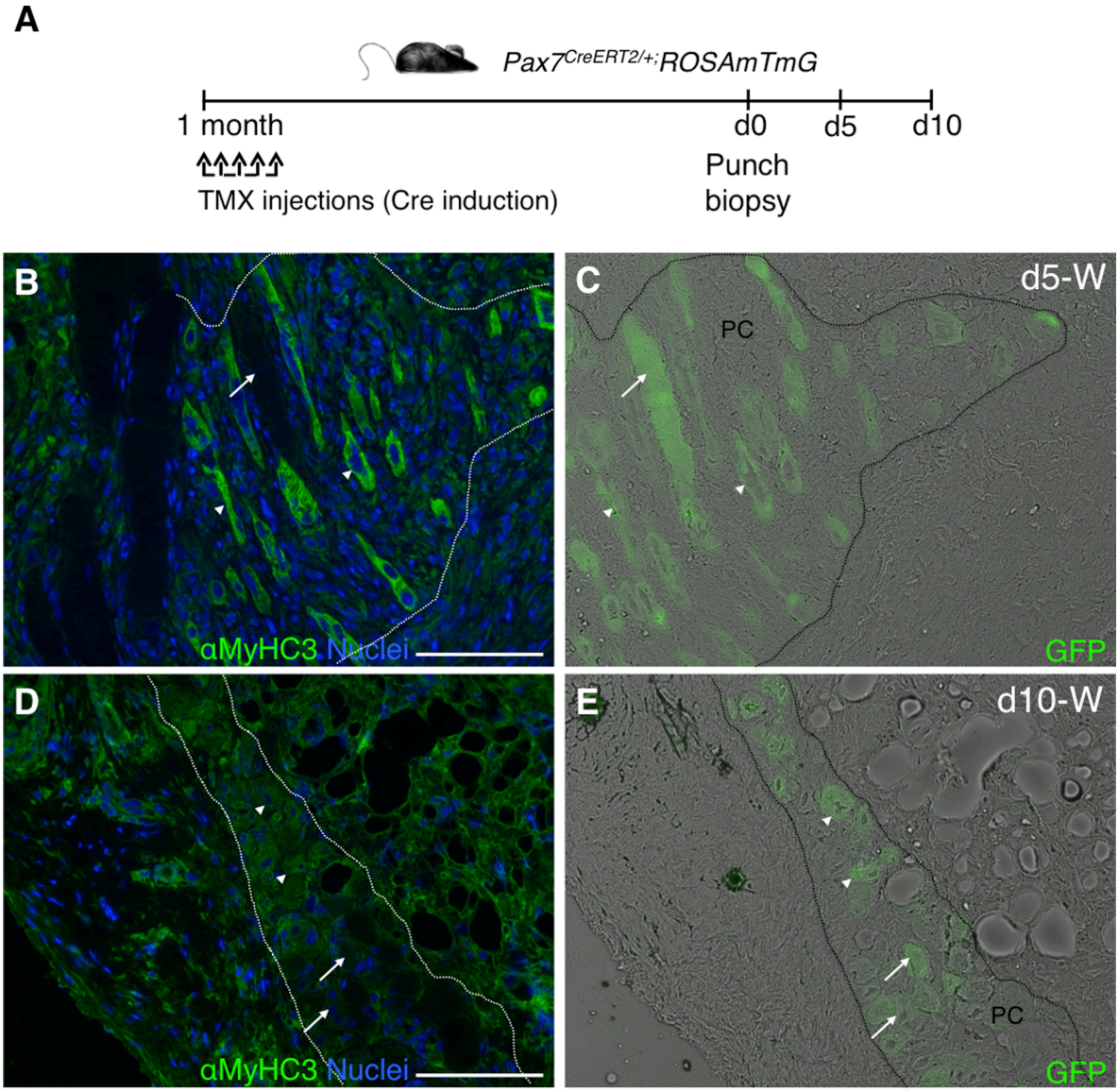

Figure S2. Presence of regenerative fibers in the *Panniculus carnosus* after wounding, related to Figure 3. (A) Outline of experimental design for the long-term induction of *Pax7* expression before punch biopsy is performed. (B-E) Histological sections of injured dorsal skin at day 5 (B-C) and at day 10 (D-E) post-wounding, were analyzed by immunofluorescence with anti-MyHC3 antibody showing regenerative fibers (B, D) and the GFP fluorescence showing *Pax7*-derived fibers (C,E). GFP+ MyHC3- cells are marked by arrows and GFP+ MyHC3+ cells are marked by arrowheads. Nuclei were counterstained with Hoechst 33258 (blue). Scale bars, 100 µm.

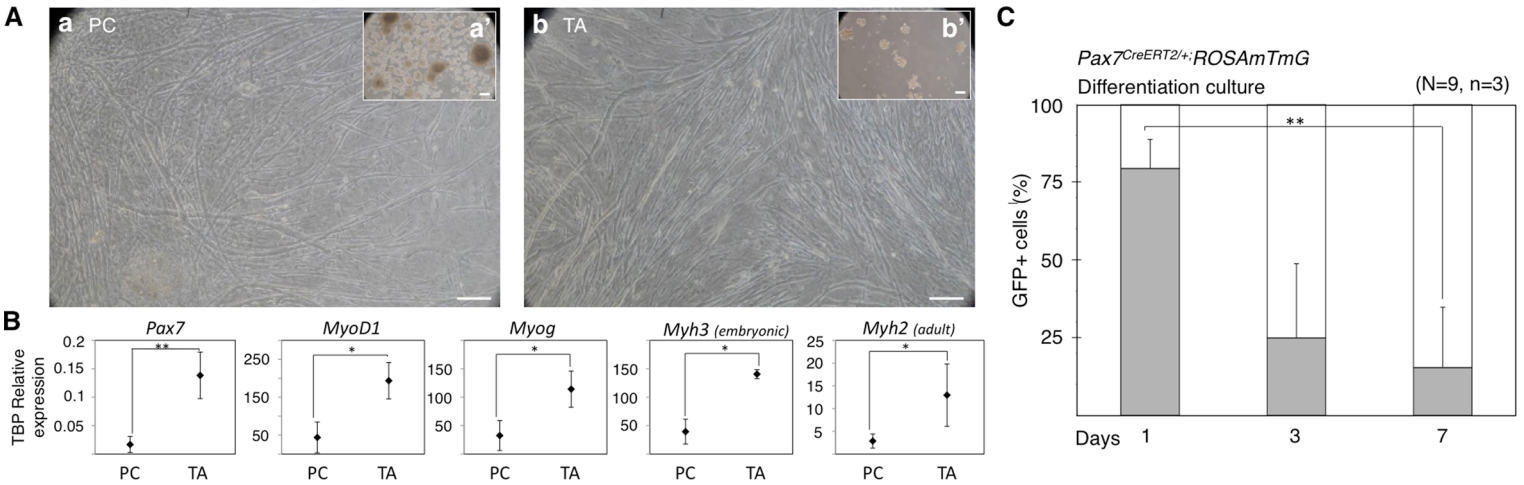

Figure S3. Comparison of limb muscle (TA)-derived and dermal muscle (PC)-derived myogenic differentiation cultures, related to Figure 5. (A) Morphologic aspects of sphere cultures of cells isolated from dermal PC muscle (a') and TA muscle (b'), and differentiated cultures of dermal PC (a) and TA muscle (b). (B) Quantitative real-time PCR (qRT-PCR) analysis for mRNA expression of myogenic markers *Pax7*, *MyoD1*, *Myogenin (Myog), MyH3 (embryonic MyHC),* and *MyH2 (adult MyHC)* in differentiated cultures from PC and TA. Expression is shown relative to *Tbp* and it is represented as the mean±SD of three independent mice. (C) Percentage of GFP+ mono- (grey bars) and multinucleated cells (white bars) at days 1, 3, and 7 of differentiation, as detected by immunofluorescence. Bars represent mean±SD. The experiments were independently replicated as specified (N=mice; n=experiments) (brackets: **=p<0.01; *=p<0.05).

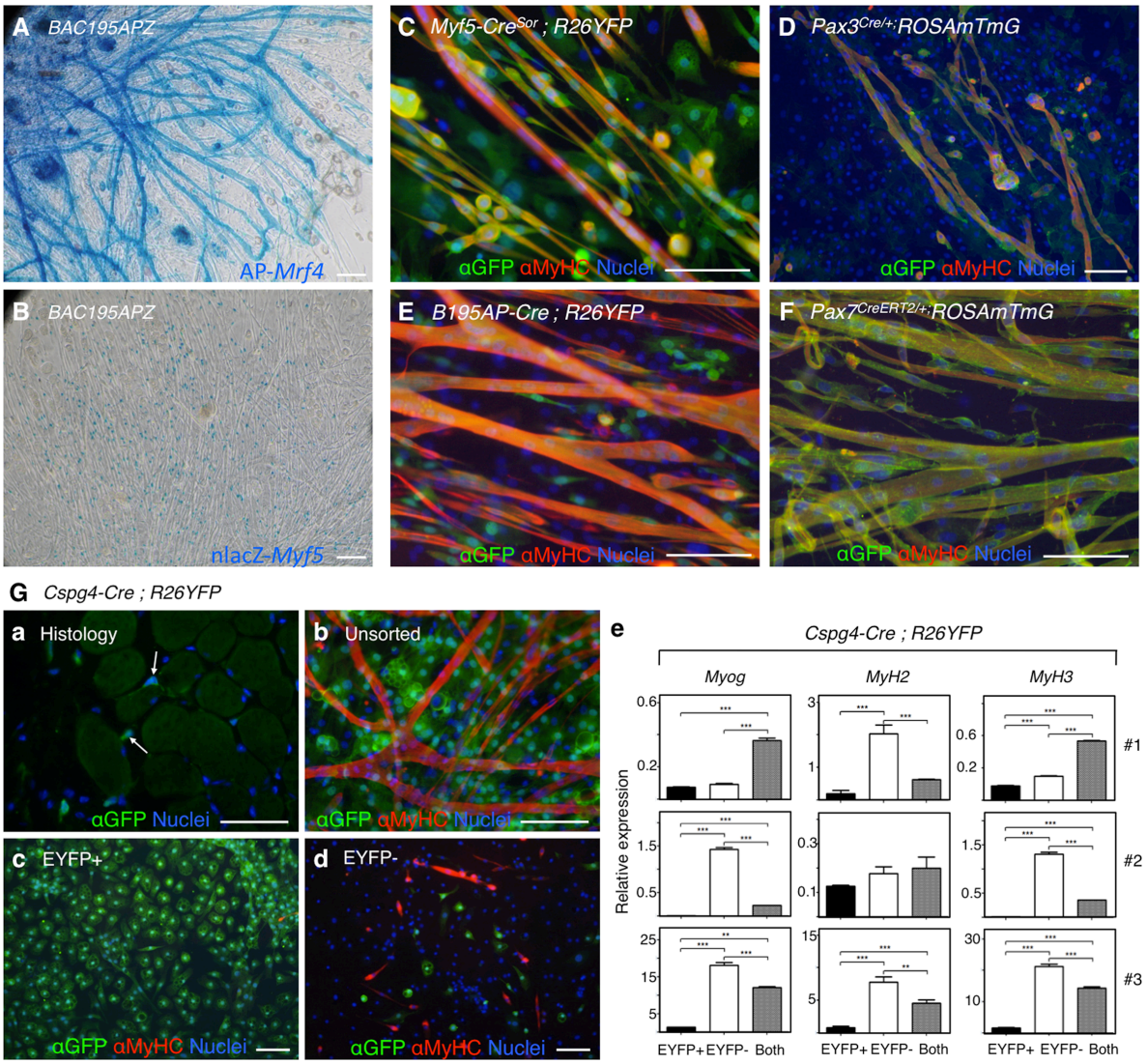

Figure S4. PC satellite cell progeny gives rise to dermis-derived myotubes, related to Figure 5. (A-B) Detection of AP-*Mrf4+* (panel A) and nlacZ-*Myf5+* (panel B) cells in differentiation cultures. (C-F) Contribution of Myf5^{SOR} (panel C), *Pax3Cre* (panel D), *B195AP-Cre* (panel E), and *Pax7^{CE}* (panel F)-derived cells to striated muscle was determined by immunofluorescence with anti-GFP (for EYFP expression), and sarcoplasmic anti-myosin heavy chain (MyHC, all fibers) antibodies. (G) Contribution of *Cspg4Cre*-derived cells to striated muscle. (a) *In situ* localization of *Cspg4*-derived cells in a histological section of dorsal skin by immunofluorescence with anti-GFP antibody. (b-d) Contribution of unsorted *Cspg4Cre*-derived cells (panel b) and FACS-sorted cell fractions [EYFP+ (panel c), EYFP- (panel d)] to striated muscle differentiation was measured by immunofluorescence with anti-GFP (for EYFP expression), and sarcoplasmic anti-myosin heavy chain (MyHC, all fibers) antibodies. Nuclei were counterstained with Hoechst 33258 (blue). (e)

Quantitative real-time PCR (qRT-PCR) analysis for mRNA expression of myogenic markers *Myogenin (Myog), MyH2 (adult MyHC)* and *MyH3 (embryonic MyHC)* from differentiated cultures of sorted cell fractions, "Both" fraction representing the mixture of EYFP+ and EYFP- sorted populations in the same percentages as in the original unsorted population. Expression is shown relative to the unsorted fraction (not shown). Bars represent mean±SD of a single experiment in which mRNA from eight mice was pooled (brackets: *p<0.05, **p<0.01, ***p<0.001). Scale bars in all immunofluorescence panels, 100 µm.

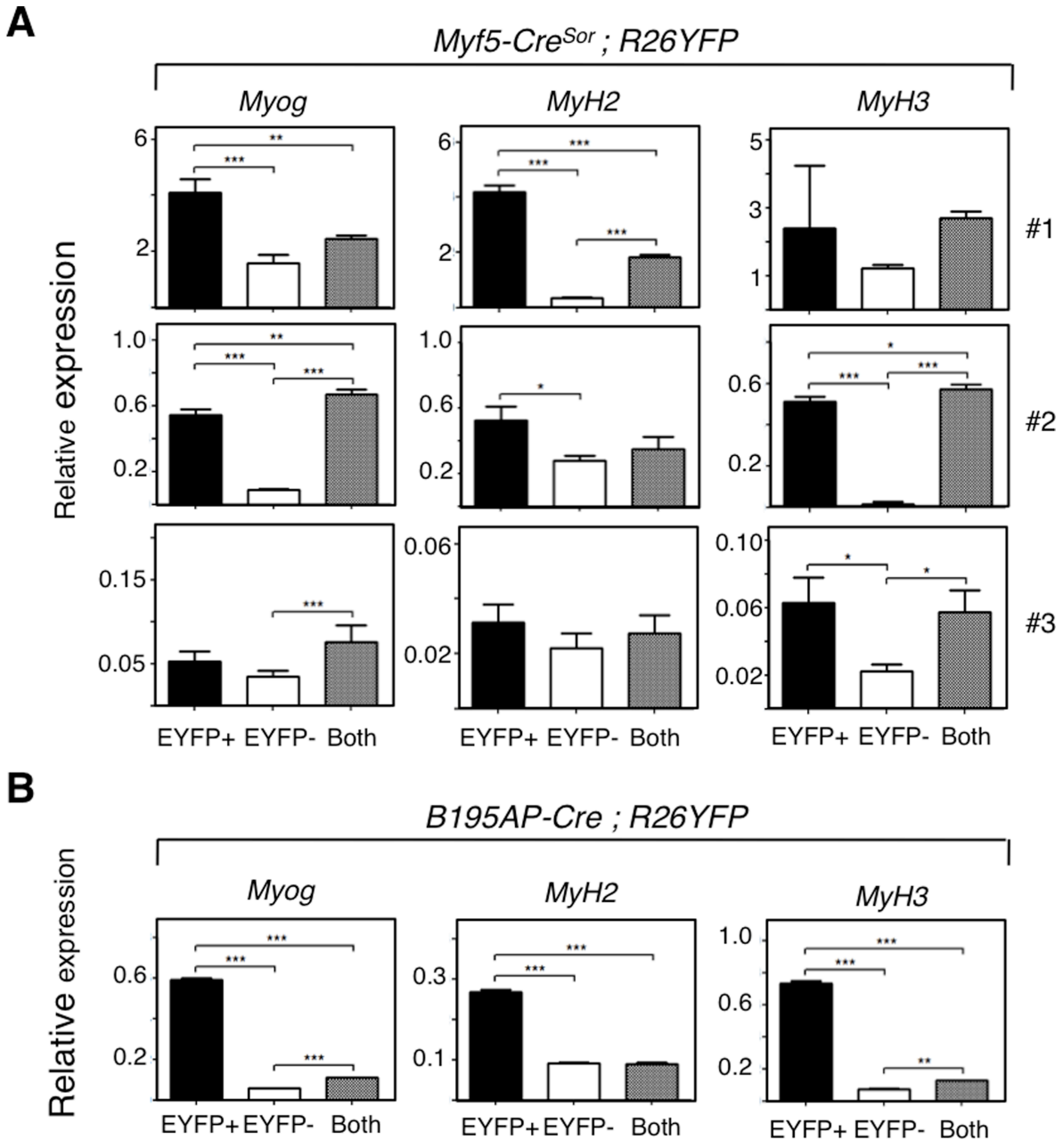

Figure S5. Quantitative contribution from *Myf5*^{SOR} and *B195AP*-traced cell lineages to striated muscle derivation, related to Figure 6. (A-B) Quantitative real-time PCR (qRT-PCR) analysis for mRNA expression of myogenic markers *Myogenin* (*Myog*), *MyH2 (adult MyHC)* and *MyH3 (embryonic MyHC)* from differentiated cultures of sorted cell fractions and "Both" fraction [representing the mixture of EYFP+ and EYFP- sorted populations in the same percentages as represented in the original cell population]. Expression is shown relative to the unsorted cell fraction (not shown). Chart bars represent mean±SD of three independent experiments (#1, #2, #3) in which mRNA from at least four mice was pooled (brackets: *p<0.05, **p<0.01, ***p<0.001).

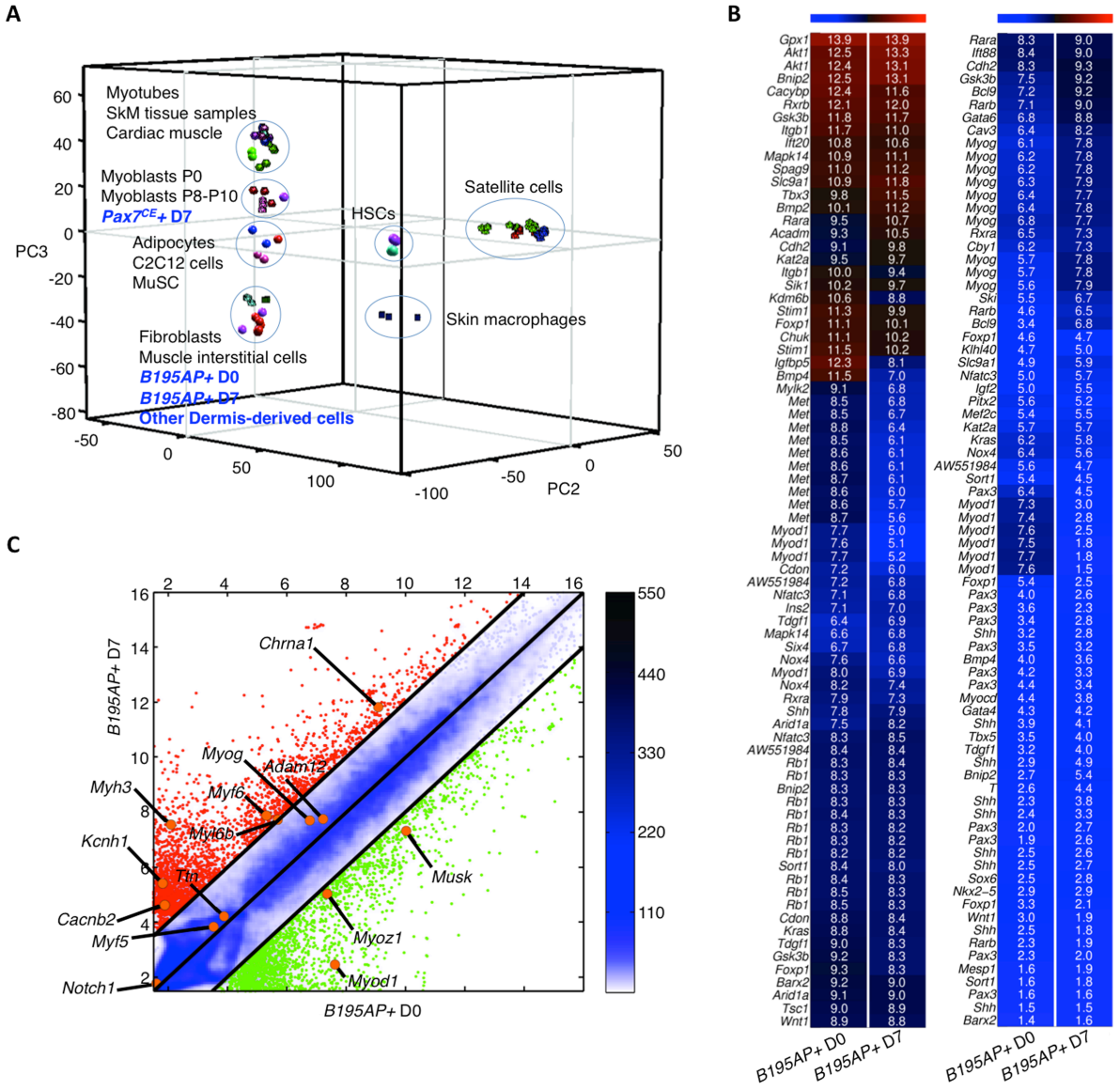

Figure S6. Transcriptomic analysis of *Myf5+* dermal myogenic precursors, related to Figure 6. Total RNAs from FACS-sorted dermal *B195AP*(+/-) and *Pax7*^{CE}(+/-) cell fractions were isolated at days 0 and 7 of proliferation culture. Total RNAs from dermal *Myf5*^{SOR}(+/-), *B195AP*(+/-) and *Cspg4*(+/-) cell fractions as well as from CD1 control mice were isolated. Since Syndecan-4 (Sdc4), a well-known satellite cell marker (Cornelison et al., 2001; Tanaka et al., 2009) was enriched in *Myf5*-EYFP+ cells (data not shown), *Myf5*^{SOR}(+/-), *B195AP*(+/-), *Cspg4*(+/-), and *CD1* control mice cells were fractionated using this marker as well. Microarray analyses were compared to database samples as detailed in Table S2. (A) Principal Component Analysis (PCA) of gene expression data. The 1st principal component (PC1) captures 47% of the gene expression variability. PC2 and PC3

capture 13 and 7.3% of the variability, respectively. (B) Heat maps showing the expression levels of the 154 probes (63 genes) associated with the GO category "striated muscle cell differentiation" in the *B195AP+* cells at day 0 (D0) and day 7 (D7). (C) Pairwise scatter plot of *B195AP+* cells at day 0 (D0) and day 7 (D7). The positions of some myogenic markers (*Myod1, Myoz1, Musk, Adam12, Myog, Ttn, Myf5, Notch1, Chrna1, Myl6b, Myf6, Myh3, Cacnb2,* and *Kcnh1*) are shown as orange dots. The color bar to the right indicates the scattering density. The gene expression levels are log2 scaled.

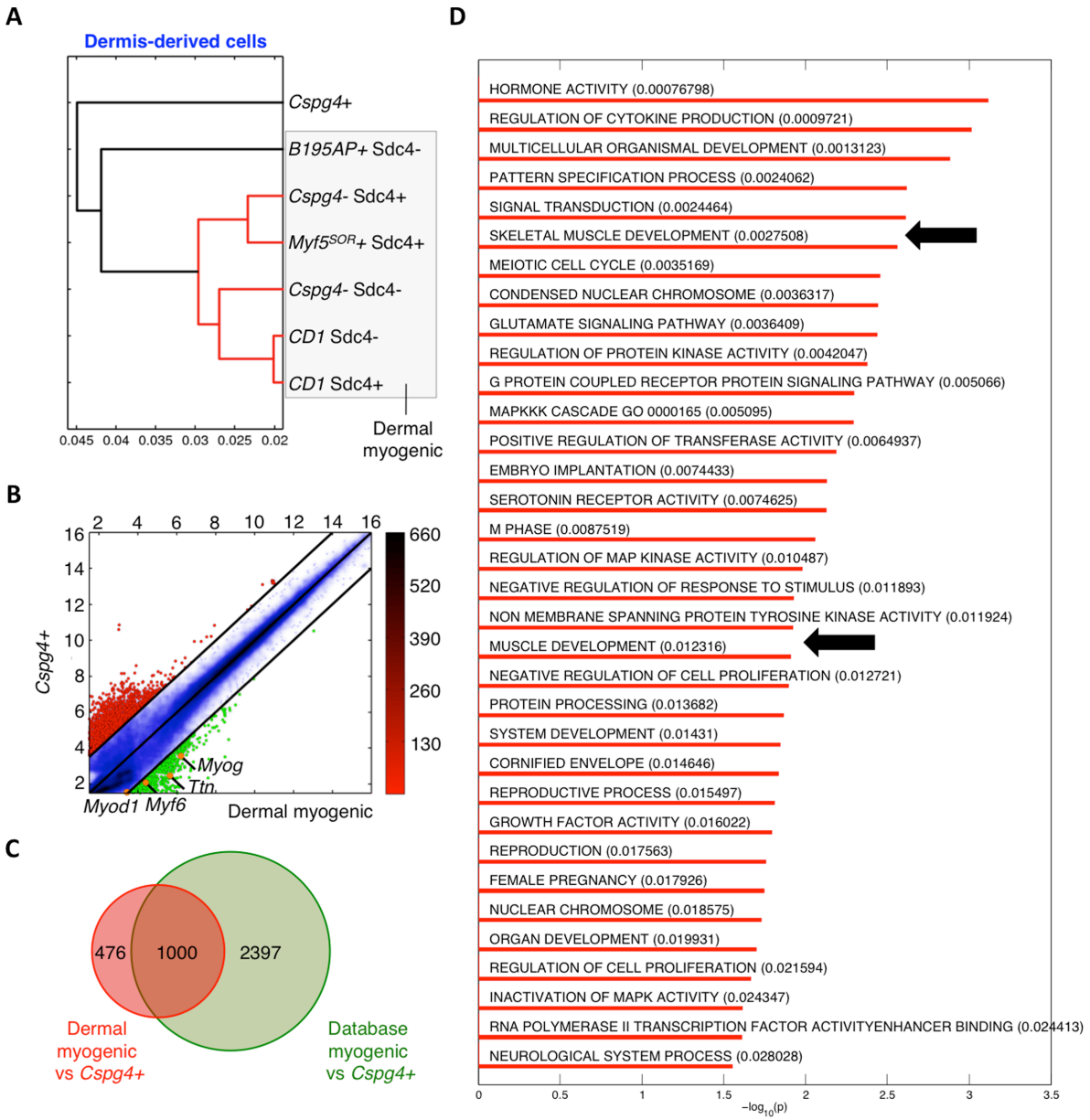

Figure S7. Transcriptomic analysis of dermal myogenic and non-myogenic precursor cell fractions, related to Figure 6. Total RNAs from dermal *Myf5*^{SOR}(+/-), *B195AP*(+/-) and *Cspg4*(+/-) cell fractions as well as from *CD1* control mice were isolated. Since Syndecan-4 (Sdc4), a well-known satellite cell marker (Cornelison et al., 2001; Tanaka et al., 2009) was enriched in *Myf5*-EYFP+ cells (data not shown), cells were fractionated using this marker as well. Microarray analyses were compared to database samples as detailed in Table S2. (A) Hierarchical clustering of samples performed using the correlation metric and the average linkage method. (B) Pairwise scatter plot. Genes upregulated in ordinates sample compared with abscissas samples are shown

in red circles; those downregulated are shown in green. The positions of some myogenic markers (*Myod1, Myf6, Ttn, Myog*) are shown as orange dots. The color bar to the right indicates the scattering density. The gene expression levels are log2 scaled. (C) Venn diagram showing overlap among (i) genes upregulated between dermal myogenic and *Cspg4+* cell fractions, and (ii) database myogenic and *Cspg4+* cell fractions. (D) Plot bar of the -log10(p) of the significant GSEA-enriched terms (p-values given in parentheses). Arrows point to muscle-related GSEA terms.

SUPPLEMENTAL TABLES

Supplemental Table S1. Mouse strains used in this study, related to Figures 1-7.

Abbreviated name	Full name	JAX stock number[1]	Charles River strain code[2]	Harlan order code[3]	Reference
B195AP^{Cre}	*BAC195AP-Cre*				This study
B195APZ	*BAC195APZ*				(Carvajal et al., 2001)
Bmi1$^{CreER/+}$	*B6;129-Bmi1$^{tm1(cre/ERT)Mrc}$/J*	010531			(Sangiorgi and Capecchi, 2008)
CD1	*Crl:CD1(ICR)*		022		
Cspg4^{Cre}	*B6;FVB-Tg(Cspg4-cre)1Akik/J*	008533			(Zhu et al., 2008)
Foxn1^{nu}	*Hsd:Athymic Nude-Foxn1^{nu}*			069(nu) 070(nu/+)	(Pantelouris, 1968)
Myf5^{CreSOR}	*B6.129S4-Myf5tm3(cre)Sor /J*	007893			(Tallquist et al., 2000)
Pax3$^{Cre/+}$	*B6;129-Pax3tm1(cre)Joe/J*	005549			(Engleka et al., 2005)
Pax3$^{GFP/+}$					(Relaix et al., 2005)
Pax3$^{IRESnLacZ/+}$					(Relaix et al., 2003)
Pax7$^{CreER2/+}$	*B6;129-Pax7tm2.1(cre/ERT2)Fan/J*	012476			(Lepper et al., 2009; Lepper and Fan, 2011; Lepper et al., 2011)
ROSAmTmG	*Gt(ROSA)26Sortm4(ACTB-tdTomato,-EGFP)Luo/J*	007676			(Muzumdar et al., 2007)
R26R	*FVB.129S4(B6)-Gt(ROSA)26Sor^{tm1Sor}/J*	009427			(Soriano, 1999)
R26R$^{GFP-DTA/+}$	*Gt(ROSA)26Sor$^{tm1(DTA)Jpmb}$/J*	006331			(Ivanova et al., 2005)
R26YFP	*B6.129X1-Gt(ROSA)26Sortm1(EYFP)Cos/J*	006148			(Srinivas et al., 2001)

[1] http://jaxmice.jax.org
[2] http://www.criver.com
[3] http://www.harlan.com

Supplemental Table S2. Arrays used for transcriptomic analyses, related to Figures S6 and S7.

GSM #	Description	Reference
GSM990708	Cardiomyocytes - 129SvEv/C57BL/6 wild type mice cardiomyocytes 16hr after PBS injection.	(Zhang et al., 2012)
GSM990709		
GSM990710		
GSM997165	Myoblastic - C2C12 myoblastic cell line.	(Davidovic et al., 2013)
GSM997166		
GSM1541931	Myoblasts P0 - C57BL/6J mice primary myoblasts in proliferation conditions at passage 0.	Carrió and Suelves, unpublished
GSM1541932		
GSM1541933		
GSM1541934	Myoblasts Prolif - C57BL/6J mice primary myoblasts in proliferation conditions at passage 8-10.	
GSM1541935		
GSM1541936		
GSM1541937	Myotubes D1 - C57BL/6J mice primary myotubes differentiation conditions at day 1.	
GSM1541938		
GSM1541939		
GSM1541940	Myotubes D2 - C57BL/6J mice primary myotubes differentiation conditions at day 2.	
GSM1541941		
GSM1541942		
GSM1541943	Myotubes D4 - C57BL/6J mice primary myotubes differentiation conditions at day 4.	
GSM1541944		
GSM1541945		
GSM1541949	Skeletal Muscle - NOD/ShiLtj mice skeletal muscle.	
GSM1541946	Quadriceps - 129Sv/C57BL/6J mice quadriceps muscle.	
GSM1541947		
GSM1541948		
GSM856087	MuSC - C57BL/6J DMD/MDX mice FACS sorted cells, CD34+/a7-integrin+/Sca1-.	Roy M Williams, unpublished
GSM856083	Muscle Interstitial - C57BL/6J DMD/MDX mice FACS sorted cells, CD34+/a7-integrin+/Sca1+.	
GSM856084		
GSM1253022	Skeletal Muscle AR97Q - C57BL/6J AR-97Q mice skeletal muscle.	(Iida et al., 2015)
GSM1253023		
GSM1253024		
GSM1299431	Satellite Young 1 - C57BL/6 2 month aged mice FACS sorted satellite cells.	(Sousa-Victor et al., 2014)
GSM1299432		
GSM1299433		
GSM1299438	Satellite Young 2 - C57BL/6 2 month aged mice FACS sorted satellite cells.	
GSM1299439		
GSM1299440		
GSM1299452	Satellite Young 3 - C57BL/6 2 month aged mice FACS sorted satellite cells.	
GSM1299453		
GSM1299454		
GSM1299458	Satellite WTBmi1 4 - FVB wild type 2 month aged mice FACS sorted satellite cells.	

GSM1299459		
GSM1299460		
GSM1299441	Satellite Old 2 - C57BL/6 23 month aged mice FACS sorted satellite cells.	
GSM1299442		
GSM1299443		
GSM1299455	Satellite Adu 3 - C57BL/6 6 month aged mice FACS sorted satellite cells.	
GSM1299456		
GSM1299457		
GSM1299434	Satellite Ger 1 - C57BL/6 28 month aged mice FACS sorted satellite cells.	
GSM1299435		
GSM1299436		
GSM1299444	Satellite Ger 2 - C57BL/6 28 month aged mice FACS sorted satellite cells.	
GSM1299445		
GSM1220789	Fibroblast - C57/Bl6-J mice tail fibroblasts cells.	(Furtado et al., 2014)
GSM1220790		
GSM1220791		
GSM1037932	Adipocytes - 3T3-L1 cultured mature adipocytes treated with physiological saline	(Chew et al., 2014)
GSM1037933		
GSM1109740	HSC-CD41- - Freshly FACS sorted HSCs from mouse bone marrow, Lin-sca1+ckit+flt3-CD41-	(Gekas and Graf, 2013)
GSM1109741		
GSM1109742		
GSM1109743	HSC-CD41+ - Freshly FACS sorted HSCs from mouse bone marrow, Lin-sca1+ckit+flt3-CD41+	
GSM1109744		
GSM1109745		
GSM1400758	Macrophages - CD1 skin resident macrophages	Castellana and Perez-Moreno, unpublished
GSM1400759		
GSM1400760		

SUPPLEMENTAL REFERENCES

Carvajal, J.J., Cox, D., Summerbell, D., and Rigby, P.W.J. (2001). A BAC transgenic analysis of the Mrf4 / Myf5 locus reveals interdigitated elements that control activation and maintenance of gene expression during muscle development. Development *1868*, 1857-1868.

Carvajal, J.J., Keith, A., and Rigby, P.W. (2008). Global transcriptional regulation of the locus encoding the skeletal muscle determination genes Mrf4 and Myf5. Genes & development *22*, 265-276.

Chew, S.H., Okazaki, Y., Nagai, H., Misawa, N., Akatsuka, S., Yamashita, K., Jiang, L., Yamashita, Y., Noguchi, M., Hosoda, K.*, et al.* (2014). Cancer-promoting role of adipocytes in asbestos-induced mesothelial carcinogenesis through dysregulated adipocytokine production. Carcinogenesis *35*, 164-172.

Cornelison, D.D., Filla, M.S., Stanley, H.M., Rapraeger, A.C., and Olwin, B.B. (2001). Syndecan-3 and syndecan-4 specifically mark skeletal muscle satellite cells and are implicated in satellite cell maintenance and muscle regeneration. Dev Biol *239*, 79-94.

Dahlqvist, C., Blokzijl, A., Chapman, G., Falk, A., Dannaeus, K., Ibanez, C.F., and Lendahl, U. (2003). Functional Notch signaling is required for BMP4-induced inhibition of myogenic differentiation. Development *130*, 6089-6099.

Davidovic, L., Durand, N., Khalfallah, O., Tabet, R., Barbry, P., Mari, B., Sacconi, S., Moine, H., and Bardoni, B. (2013). A novel role for the RNA-binding protein FXR1P in myoblasts cell-cycle progression by modulating p21/Cdkn1a/Cip1/Waf1 mRNA stability. PLoS genetics *9*, e1003367.

DeChiara, T.M., Bowen, D.C., Valenzuela, D.M., Simmons, M.V., Poueymirou, W.T., Thomas, S., Kinetz, E., Compton, D.L., Rojas, E., Park, J.S.*, et al.* (1996). The receptor tyrosine kinase MuSK is required for neuromuscular junction formation in vivo. Cell *85*, 501-512.

Engleka, K.A., Gitler, A.D., Zhang, M., Zhou, D.D., High, F.A., and Epstein, J.A. (2005). Insertion of Cre into the Pax3 locus creates a new allele of Splotch and identifies unexpected Pax3 derivatives. Dev Biol *280*, 396-406.

Furtado, M.B., Costa, M.W., Pranoto, E.A., Salimova, E., Pinto, A.R., Lam, N.T., Park, A., Snider, P., Chandran, A., Harvey, R.P.*, et al.* (2014). Cardiogenic genes expressed in cardiac fibroblasts contribute to heart development and repair. Circulation research *114*, 1422-1434.

Gekas, C., and Graf, T. (2013). CD41 expression marks myeloid-biased adult hematopoietic stem cells and increases with age. Blood *121*, 4463-4472.

Halevy, O., and Lerman, O. (1993). Retinoic acid induces adult muscle cell differentiation mediated by the retinoic acid receptor-alpha. Journal of cellular physiology *154*, 566-572.

Iida, M., Katsuno, M., Nakatsuji, H., Adachi, H., Kondo, N., Miyazaki, Y., Tohnai, G., Ikenaka, K., Watanabe, H., Yamamoto, M.*, et al.* (2015). Pioglitazone suppresses neuronal and muscular degeneration caused by polyglutamine-expanded androgen receptors. Human molecular genetics *24*, 314-329.

Ivanova, A., Signore, M., Caro, N., Greene, N.D., Copp, A.J., and Martinez-Barbera, J.P. (2005). In vivo genetic ablation by Cre-mediated expression of diphtheria toxin fragment A. Genesis *43*, 129-135.

Lepper, C., Conway, S., and Fan, C. (2009). Adult satellite cells and embryonic muscle progenitors have distinct genetic requirements. Nature *460*, 627-631.

Lepper, C., and Fan, C.-m. (2011). Inducible lineage tracing of Pax7-descendant cells reveals embryonic origin of adult satellite cells. Genesis *48*, 424-436.

Lepper, C., Partridge, T.a., and Fan, C.-M. (2011). An absolute requirement for Pax7-positive satellite cells in acute injury-induced skeletal muscle regeneration. Development *138*, 3639-3646.

Lovett, F.A., Gonzalez, I., Salih, D.A., Cobb, L.J., Tripathi, G., Cosgrove, R.A., Murrell, A., Kilshaw, P.J., and Pell, J.M. (2006). Convergence of Igf2 expression and adhesion signalling via RhoA and p38 MAPK enhances myogenic differentiation. J Cell Sci *119*, 4828-4840.

Muzumdar, M., Tasic, B., Miyamichi, K., Li, L., and Luo, L. (2007). A global double-fluorescent Cre reporter mouse. Genesis *605*, 593-605.

Ono, Y., Calhabeu, F., Morgan, J.E., Katagiri, T., Amthor, H., and Zammit, P.S. (2011). BMP signalling permits population expansion by preventing premature myogenic differentiation in muscle satellite cells. Cell death and differentiation *18*, 222-234.

Pantelouris, E.M. (1968). Absence of thymus in a mouse mutant. Nature *217*, 370-371.

Relaix, F., Polimeni, M., Rocancourt, D., Ponzetto, C., Schafer, B.W., and Buckingham, M. (2003). The transcriptional activator PAX3-FKHR rescues the defects of Pax3 mutant mice but induces a myogenic gain-of-function phenotype with ligand-independent activation of Met signaling in vivo. Genes & development *17*, 2950-2965.

Relaix, F., Rocancourt, D., Mansouri, A., and Buckingham, M. (2005). A Pax3/Pax7-dependent population of skeletal muscle progenitor cells. Nature *435*, 948-953.

Rozwadowska, N., Kolanowski, T., Wiland, E., Siatkowski, M., Pawlak, P., Malcher, A., Mietkiewski, T., Olszewska, M., and Kurpisz, M. (2013). Characterisation of nuclear architectural alterations during in vitro differentiation of human stem cells of myogenic origin. PLoS One *8*, e73231.

Sambasivan, R., Comai, G., Le Roux, I., Gomes, D., Konge, J., Dumas, G., Cimper, C., and Tajbakhsh, S. (2013). Embryonic founders of adult muscle stem cells are primed by the determination gene Mrf4. Dev Biol *381*, 241-255.

Sangiorgi, E., and Capecchi, M.R. (2008). Bmi1 is expressed in vivo in intestinal stem cells. Nature genetics *40*, 915-920.

Sharples, A.P., Al-Shanti, N., Lewis, M.P., and Stewart, C.E. (2011). Reduction of myoblast differentiation following multiple population doublings in mouse C2 C12 cells: a model to investigate ageing? Journal of cellular biochemistry *112*, 3773-3785.

Sousa-Victor, P., Gutarra, S., Garcia-Prat, L., Rodriguez-Ubreva, J., Ortet, L., Ruiz-Bonilla, V., Jardi, M., Ballestar, E., Gonzalez, S., Serrano, A.L*., et al.* (2014). Geriatric muscle stem cells switch reversible quiescence into senescence. Nature *506*, 316-321.

Srinivas, S., Watanabe, T., Lin, C.S., William, C.M., Tanabe, Y., Jessell, T.M., and Costantini, F. (2001). Cre reporter strains produced by targeted insertion of EYFP and ECFP into the ROSA26 locus. BMC developmental biology *1*, 4.

Stern-Straeter, J., Bonaterra, G.A., Hormann, K., Kinscherf, R., and Goessler, U.R. (2009). Identification of valid reference genes during the differentiation of human myoblasts. BMC molecular biology *10*, 66.

Subramanian, A., Tamayo, P., Mootha, V.K., Mukherjee, S., Ebert, B.L., Gillette, M.A., Paulovich, A., Pomeroy, S.L., Golub, T.R., Lander, E.S*., et al.* (2005). Gene set enrichment analysis: a knowledge-based approach for interpreting genome-wide expression profiles. Proceedings of the National Academy of Sciences of the United States of America *102*, 15545-15550.

Swaminathan, S., Ellis, H.M., Waters, L.S., Yu, D., Lee, E.C., Court, D.L., and Sharan, S.K. (2001). Rapid engineering of bacterial artificial chromosomes using oligonucleotides. Genesis *29*, 14-21.

Tallquist, M.D., Weismann, K.E., Hellstrom, M., and Soriano, P. (2000). Early myotome specification regulates PDGFA expression and axial skeleton development. Development *127*, 5059-5070.

Tanaka, K.K., Hall, J.K., Troy, A.A., Cornelison, D.D., Majka, S.M., and Olwin, B.B. (2009). Syndecan-4-expressing muscle progenitor cells in the SP engraft as satellite cells during muscle regeneration. Cell Stem Cell *4*, 217-225.

Voronova, A., Coyne, E., Al Madhoun, A., Fair, J.V., Bosiljcic, N., St-Louis, C., Li, G., Thurig, S., Wallace, V.A., Wiper-Bergeron, N*., et al.* (2013). Hedgehog signaling regulates MyoD expression and activity. The Journal of biological chemistry *288*, 4389-4404.

Zhang, S., Liu, X., Bawa-Khalfe, T., Lu, L.S., Lyu, Y.L., Liu, L.F., and Yeh, E.T. (2012). Identification of the molecular basis of doxorubicin-induced cardiotoxicity. Nat Med *18*, 1639-1642.

Zhu, X., Hill, R.A., and Nishiyama, A. (2008). NG2 cells generate oligodendrocytes and gray matter astrocytes in the spinal cord. Neuron glia biology *4*, 19-26.